Available online at www.sciencedirect.com

ScienceDirect

Procedia Engineering 81 (2014) 736 – 741

Procedia Engineering

www.elsevier.com/locate/procedia

11th International Conference on Technology of Plasticity, ICTP 2014, 19-24 October 2014, Nagoya Congress Center, Nagoya, Japan

Predicting effect of temperature, strain rate and strain path changes on forming limit of lightweight sheet metal alloys

Omer El Fakir, LiLiang Wang*, Daniel Balint, John P. Dear, Jianguo Lin

Department of Mechanical Engineering, City and Guilds Building, Imperial College London, SW7 2BX, UK

Abstract

With the advent of novel hot stamping technologies to produce increasingly complex components, conventional FLDs, which are usually only determined at a constant temperature, strain rate and strain path, are unable to provide an accurate definition of formability. This is particularly the case with the solution Heat treatment, Forming and in-die Quenching (HFQ) process. In this work, a viscoplastic constitutive model was developed to predict the flow stress and formability of a sheet metal alloy undergoing temperature, strain rate and strain path changes. The capability of the proposed model was demonstrated by presenting the effect of these varying conditions on the stress-strain curves and FLDs of the aluminium alloy AA5754.

Selection and peer-review under responsibility of the Department of Materials Science and Engineering, Nagoya University

Keywords: Forming limit diagrams; Constitutive modelling; Aluminium alloy; AA5754; Hot stamping; HFQ

1. Introduction

Forming limit diagrams (FLDs) are an essential tool in the finite element (FE) modelling of forming processes, as they indicate the level of deformation that can occur in a sheet metal alloy before fracture takes place. They are determined experimentally for constant temperatures, strain paths and strain rates, by measuring the limit strains of specimens formed using stretch-forming tests (Ayres and Wenner, 1979; Naka et al., 2001). Sheet metal formability has been shown to differ with varying temperature, strain rate and strain path (Hsu et al., 2008; Hsu et

* Corresponding author. Prof. Lin, Tel.: +44 20 7594 7082; Dr. Wang,Tel: +44 20 7594 3648.
E-mail address: jianguo.lin@imperial.ac.uk, liliang.wang@imperial.ac.uk

Selection and peer-review under responsibility of the Department of Materials Science and Engineering, Nagoya University
doi:10.1016/j.proeng.2014.10.069

al., 2006; Stoughton and Yoon, 2012), however due to the time and resources required to generate a single FLD, it would not be realistic to produce one for every possible condition that occurs in a forming process.

With the tremendous growth in the use of lightweight alloys in vehicle structures to curb CO_2 emissions (Casadei and Broda, 2007; Lutsey, 2010), the application of warm and hot stamping technologies to produce components from these alloys has been expanding; the limited formability at room temperature necessitates the use of elevated temperatures (Mohamed et al., 2012; Toros et al., 2008; Wang et al., 2011). One such technology is the solution Heat treatment, Forming, and in-die Quenching process, in which the sheet metal is solutionized before forming at a high speed in a cold die (Lin and Dean, 2005; Mohamed et al., 2012; Wang et al., 2011). Experimentally determined FLDs would no longer be applicable to such a process, due to the varying temperature, strain rate and strain path that different regions of the sheet metal experience during forming. In effect, each point of a formed component would have its own loading history, and theoretically, a unique FLD would be required for each point. A sensible FLD prediction model is therefore essential.

In the present study, a viscoplastic constitutive model was developed to predict the stress-strain relationships and FLDs for a lightweight sheet metal alloy undergoing temperature, strain rate and strain path changes during deformation. Dislocation density-based hardening constitutive equations were utilized to model the flow stress evolution, taking into account the thermo-mechanical history of the deformation, with the anisotropic behaviour of the sheet metal described by the Hosford yield criterion. A physically based damage model was implemented to predict fracture. The model was calibrated using the results of uniaxial tensile tests and formability tests conducted on the aluminium alloy AA5754. The effect of varying temperature, strain rate and strain path on the FLD was then presented.

2. Methods

2.1. Modeling details

At the elevated temperatures that a sheet metal experiences during warm or hot stamping, the microstructure and behaviour will vary throughout the process (Lin and Dean, 2005; Lin and Liu, 2003); a set of viscoplastic constitutive equations utilizing dislocation density based hardening laws was hence implemented to accurately model the deformation. These equations were combined with a physically based damage model to predict the final failure of the material. It is assumed that there exists an initial imperfection in the material, denoted zone B, where the thickness is slightly lower than the rest of the material, denoted zone A (Marciniak and Kuczyński, 1967). The initial size of this imperfection is given by f_0, and is the ratio of the thickness in zone B to A; its value was calibrated using experimental FLDs. As deformation progresses, the imperfect factor f (Equation 1) decreases, and strain becomes localized at zone B; failure occurs when the ratio of strains in zone B to A approaches a critical value, shown in Eq. (2)**.**

$$f = f_0 \exp(\varepsilon_{3B} - \varepsilon_{3A}), \tag{1}$$

$$\frac{d\varepsilon_{1B}}{d\varepsilon_{1A}} \geq 10, or \frac{d\varepsilon_{3B}}{d\varepsilon_{3A}} \geq 10. \tag{2}$$

The different points along the FLD representing different strain conditions were calculated by varying the ratio between the minor and major strain in zone A. This ratio, denoted β, has a value of -0.5 for the uniaxial condition, and a value of 1 in the biaxial condition. Deformation in zone B was then deduced from minor strain compatibility with zone A at their interface (Equation 3), and by ensuring that Eq. (4) was satisfied throughout the deformation process.

$$\varepsilon_{2A} = \varepsilon_{2B}, \tag{3}$$

$$\sigma_{1A} = f\sigma_{1B}. \tag{4}$$

All the following equations had to therefore be solved simultaneously for both zone A and B. The viscoplastic flow rule is shown in Eq. (5), and is a function of the flow stress and the isotropic hardening variable, R (Eq. (6)).

This in itself is a function of the normalized dislocation density (Eq. (7)), which accounts for the accumulation and annihilation of dislocations during deformation; hence 'R' captures the effect of hardening due to dislocation pile-up and entanglement (Lin and Dean, 2005). The anisotropic nature of the sheet material was represented by the Hosford yield function, shown in Eq. (9) (Hosford, 1985). The constant a is set to 6 for FCC metals, while R_1 and R_2 are the longitudinal and transverse r-values respectively, determined from tensile tests.

$$\dot{\bar{\varepsilon}}_{P(A,B)} = \left(\frac{\bar{\sigma}_{(A,B)} - R_{(A,B)} - k}{K} \right)^{n_1}, \tag{5}$$

$$R_{(A,B)} = B\bar{\rho}^{0.5}_{(A,B)}, \tag{6}$$

$$\dot{\bar{\rho}}_{(A,B)} = A(1-\bar{\rho}_{(A,B)})\dot{\bar{\varepsilon}}_{P(A,B)} - C\bar{\rho}^{n_2}_{(A,B)}, \tag{7}$$

$$\bar{\sigma}_{(A,B)} = E(\bar{\varepsilon}_{(A,B)} - \bar{\varepsilon}_{\mathrm{P}(A,B)}), \tag{8}$$

$$R_2\sigma^a_{1(A,B)} + R_1\sigma^a_{2(A,B)} + R_1R_2(\sigma_{1(A,B)} - \sigma_{2(A,B)})^a = R_2(R_1+1)\bar{\sigma}^a_{(A,B)}. \tag{9}$$

where k, K, n_1, B, A, n_2 and E are temperature-dependent material constants calibrated using the results of uniaxial tension tests. The equations were solved until one of the failure conditions was satisfied. The minor and major strains in zone A at failure were hence the limit strains for that particular β value; by combining the limit strains for each β value, a FLD for a constant temperature, strain rate and strain path could be constructed. The use of a time integration procedure also enabled the effect on the FLD of time dependent phenomena and process conditions, such as the varying temperatures, strain rates and strain paths in a hot stamping process, to be captured.

2.2. Experimental details

Uniaxial tension tests were conducted on the aluminium alloy AA5754 at different temperatures and strain rates. Strains rates of 0.001, 0.1 and 1/s, at temperatures of 200, 250 and 300 °C, were tested, using a high rate Instron testing machine with an integrated furnace; strain was measured through DIC techniques using ARAMIS software, provided by GOM. The results were used to calibrate the constants of the constitutive equations. The formability of the material was also assessed using dome tests (Shi et al., 2012), following the international standard for the determination of forming limit curves (ISO, 2008). Waisted circular blanks with central shafts of different widths were tested, each representing a different strain path, at different temperatures and forming speeds. The generated FLDs were then also used to calibrate the material model, by varying the f_0 value (Eq. (1)).

3. Results and discussion

Fig. 1(a) shows the close agreement that was achieved between the flow stresses predicted using the material model (solid line) and the experimental results (symbols), for different temperatures, at a strain rate of 1 /s. The viscoplastic effect was also accurately modelled, as shown by the close agreement between the predicted and experimental flow stress in Fig. 1(b) for different strain rates, at a temperature of 250 °C.

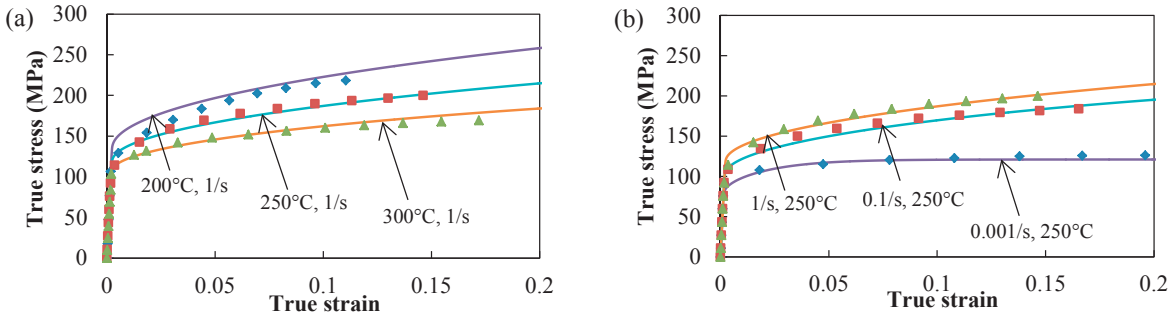

Fig. 1. Comparison between the predicted (lines) and experimental (symbols) stress-strain curves at different temperatures (a), and different strain rates (b).

With the material model for AA5754 calibrated and verified using the results of the uniaxial tension tests, it was then applied in the prediction of FLDs for the material. Fig. 2 shows close agreement between the predicted and experimental FLDs at temperatures of 200 and 300 °C, at a forming speed of 75 mm/s. The parallel flow stress curves shown in Figure 1(a) indicate that the strain hardening of AA5754 at 200 and 300 °C is almost the same. However, the strain rate hardening coefficient ($1/n_1$ in Eq. (5)) increased from 0.078 at 200 °C to 0.125 at 300 °C. Therefore, the pronounced strain rate hardening effect at higher temperatures led to the increased formability. In particular, the higher strain rate in zone B would increase the strength difference between zone A and zone B, limiting the strain ratios between them, and therefore delaying the onset of necking at zone B. The effect of a quenching rate of 50 °C/s being applied from an initial temperature of 300 °C is also presented; as expected, the resulting FLD is lower, indicating a drop in formability as a result of temperature decreasing.

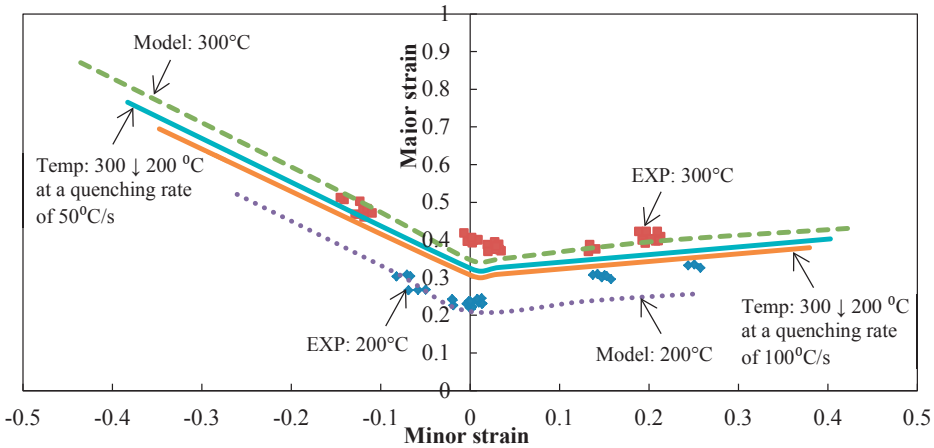

Fig. 2. Predicted and experimental FLDs at temperatures of 200 and 300°C, at a speed of 75 mm/s.

Fig. 3 shows close agreement between the predicted and experimental FLDs at forming speeds of 20 and 300 mm/s, at a temperature of 250 °C. Both strain hardening and strain rate hardening enhance formability. Strain hardening is more pronounced at low temperature conditions, while strain rate hardening is the dominant factor at higher temperatures. Hence at the onset of strain localization in zone B, and the resulting steep increase in strain rate, the strength in this region is increased, delaying the onset of necking; at 250 °C the formability is therefore higher when the strain rate is lower. The effect of a strain rate reduction to 0.25 /s being applied from an initial

strain rate of 3.5 /s is also presented; as expected, the resulting FLD is higher, indicating an improvement in formability as a result of strain rate decreasing.

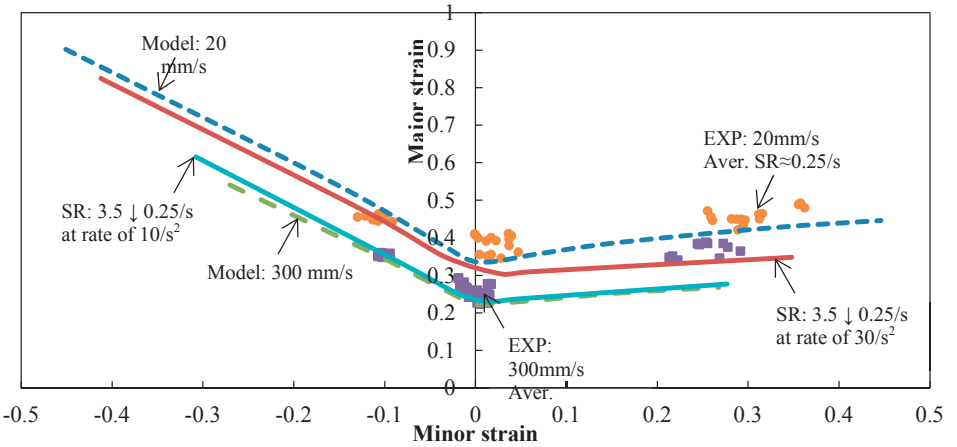

Fig. 3. Predicted and experimental FLDs at forming speeds of 20 and 300 mm/s, at a temperature of 250 °C.

A change in strain path on the FLD of AA5754 was also successfully captured, as shown in Fig. 4. Uniaxial pre-stretching enhanced the formability of the material during biaxial straining, while biaxial pre-stretching enhanced the formability of the material during uniaxial straining. This is consistent with many previous research findings, such as those of Graf and Hosford in (Graf and Hosford, 1993) and (Graf and Hosford, 1994).

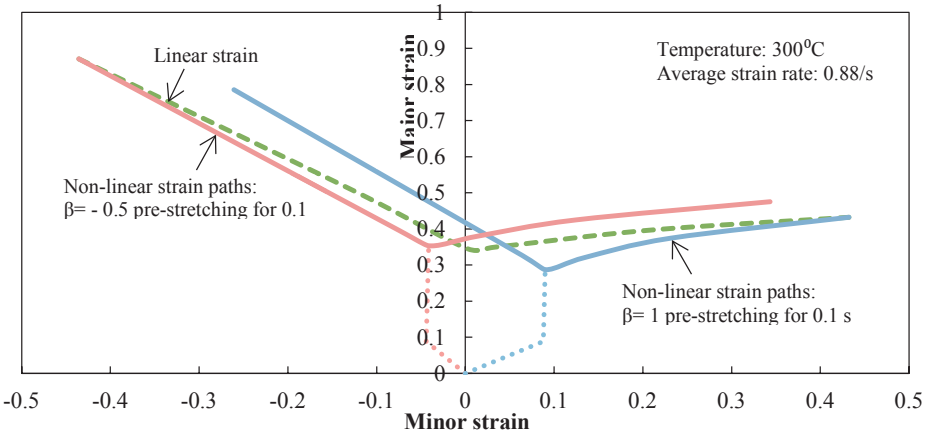

Fig. 4. Effect of change in strain path on the FLD, at temperature of 300°C and average strain rate of 0.88/s.

Although stress based forming limit curves (FLSCs) have the benefit of being almost path-independent (Yoshida et al., 2007), for hot stamping processes, traditional strain based FLCs are probably more effective; in FLSCs, each stress value may not have a corresponding unique strain value, making it more difficult to define a stress limit for necking. Also, the integration of strain with a small time increment is perhaps more suitable for the prediction of forming limits when loading history effects are pronounced.

4. Conclusion

A FLD prediction model was presented and successfully validated using experimental results from uniaxial tension and formability tests on the aluminium alloy AA5754. The ability of the model to capture time dependent

phenomena was also demonstrated, with obvious effects on the material's properties as a result of a change in temperature, strain rate and strain path. The model's capability will be further verified by comparing the measured failure strains from a point on an actual hot formed component, to the predicted forming limit at that point taking into account its temperature, strain rate and loading history. This will highlight the value of using such a model in FE forming process simulations, to ensure sensible components and forming tool design, and to select the optimal process parameters and appropriate material to produce a given sheet metal component successfully.

Acknowledgements

The authors gratefully acknowledge the support from the EPSRC (Grant Ref: EP/I038616/1) for TARF-LCV: Towards Affordable, Closed-Loop Recyclable Future Low Carbon Vehicle Structures.

References

Ayres, R., Wenner, M., 1979. Strain and strain-rate hardening effects in punch stretching of 5182-0 aluminum at elevated temperatures. MTA 10, 41-46.

Casadei, A., Broda, R., 2007. Impact of Vehicle Weight Reduction on Fuel.

Economy for Various Vehicle Architectures. Ricardo.

Graf, A., Hosford, W., 1993. Effect of changing strain paths on forming limit diagrams of Al2008-T4. Metallurgical Transactions a-Physical Metallurgy and Materials Science 24, 2503-2512.

Graf, A., Hosford, W., 1994. The influence of strain-path changes on forming limit diagrams of Al6111 T-4. International Journal of Mechanical Sciences 36, 897-910.

Hosford, W.F., 1985. Comments on anisotropic yield criteria. International Journal of Mechanical Sciences 27, 423-427.

Hsu, E., Carsley, J.E., Verma, R., 2008. Development of forming limit diagrams of aluminum and magnesium sheet alloys at elevated temperatures. J. of Materi Eng and Perform 17, 288-296.

Hsu, E., Szpunar, J.A., Verma, R., 2006. Effect of Temperature and Strain Rate on Formability of AZ31 Magnesium Sheet Alloy. SAE International.

ISO, 2008. Metallic materials -- Sheet and strip -- Determination of forming-limit curves -- Part 2: Determination of forming-limit curves in the laboratory.

Lin, J., Dean, T.A., 2005. Modelling of microstructure evolution in hot forming using unified constitutive equations. J. Mater. Process. Technol. 167, 354-362.

Lin, J., Liu, Y., 2003. A set of unified constitutive equations for modelling microstructure evolution in hot deformation. J. Mater. Process. Technol. 143, 281-285.

Lutsey, N.P., 2010. Review of technical literature and trends related to automobile mass-reduction technology. Institute of Transportation Studies, UC Davis.

Marciniak, Z., Kuczyński, K., 1967. Limit strains in the processes of stretch-forming sheet metal. International Journal of Mechanical Sciences 9, 609-620.

Mohamed, M.S., Foster, A.D., Lin, J.G., Balint, D.S., Dean, T.A., 2012. Investigation of deformation and failure features of AA6082: Experimentation and modelling. Int. J. Mach. Tools Manuf. 53, 27-38.

Naka, T., Torikai, G., Hino, R., Yoshida, F., 2001. The effects of temperature and forming speed on the forming limit diagram for type 5083 aluminum-magnesium alloy sheet. J. Mater. Process. Technol. 113, 648-653.

Shi, Z., Wang, Y., Lin, J., Dean, T.A., Balint, D., Stanton, M., Watson, D., 2012. An Investigation, Using Standard Experimental Techniques, to Determine FLCs at Elevated Temperature for Aluminium Alloys, The 3rd International Conference on New Forming Technology, Aug. 26-28, 2012, Harbin, China.

Stoughton, T.B., Yoon, J.W., 2012. Path independent forming limits in strain and stress spaces. Int. J. Solids Struct. 49, 3616-3625.

Toros, S., Ozturk, F., Kacar, I., 2008. Review of warm forming of aluminum-magnesium alloys. J. Mater. Process. Technol. 207, 1-12.

Wang, L., Strangwood, M., Balint, D., Lin, J., Dean, T.A., 2011. Formability and failure mechanisms of AA2024 under hot forming conditions. Mater. Sci. Eng. A-Struct. Mater. Prop. Microstruct. Process. 528, 2648-2656.

Yoshida, K., Kuwabara, T., Kuroda, M., 2007. Path-dependence of the forming limit stresses in a sheet metal. International Journal of Plasticity 23, 361-384.